Energy Consumption Optimization for UAV Base Stations with Wind Compensation

Marek Ruzicka, Zdenek Becvar, *Senior Member, IEEE*, Juraj Gazda

***Abstract*—In this letter, an energy-efficient algorithm for positioning of unmanned aerial vehicle-based base stations (UAV-BSs) is presented. The objective is to reduce the propulsion power consumption of UAV-BSs while not compromising the communication capacity of user equipments (UEs). As a significant step beyond state-of-the-art, we consider an effect of wind. To this end, we develop a new model of a propulsion energy consumption for the UAV-BSs reflecting an impact of wind. Furthermore, we propose a novel algorithm based on an ensemble learning optimizing the 3D trajectory of UAV-BSs over time in realistic environment with wind to reduce the propulsion energy consumption. The results show that the proposed approach reduces the propulsion energy consumption of UAV-BSs by up to 47% with only a negligible degradation in the UEs capacity compared to state-of-the-art works.**

***Index Terms*—UAV base station, energy consumption, wind, modeling, ensemble learning, machine learning**

I. Introduction

The base stations mounted on unmanned aerial vehicles (UAV-BSs) represent a promising solutions offering a connectivity to user equipments (UEs) during emergency or temporary peak traffic conditions. The major limitation related to a deployment of the UAV-BS is the battery capacity and, consequently, operational time. The available battery capacity is shared mainly by communication (transmission power), and flying (propulsion power).

Solutions targeting to reduce the transmission power of UAV-BSs typically aim to determine positions of the UAV-BSs. For example, in [1], the authors propose the optimal UAV-BSs positioning based on the circle placement problem to maximize the number of covered UEs. Furthermore, successive convex approximation for the UAV-BS deployment considering different transmission power allocated to the UEs is adopted in [2]. Downlink power control for a fleet of UAV-BSs is considered in [3]. However, in practical deployments of the rotary-wing UAV-BSs, the transmission power is few orders of magnitude lower than the propulsion power due to a highly dynamic and energy draining UAV rotors [4]. Hence, the propulsion power optimization is a key challenge.

The propulsion power optimization is addressed, e.g., in [5], [6], where the closed form solution for the UAV-BS trajectory is derived. In [7], the authors adopt multi-agent reinforcement learning to solve cooperatively the multi-criteria optimization problem involving the propulsion power reduction. In real-world outdoor applications of the UAV-BSs, a wind is always present and a mutual relation of directions of the wind and of the UAV-BS's movement influence notably the propulsion energy consumed by the UAV-BS. Nevertheless, up to our best knowledge, there is no work that would analyze an impact of the wind or even take an impact of the wind into account in the UAV-BS's trajectory design.

Hence, in this paper, we minimize the propulsion energy consumption of the UAV-BSs serving stationary/slowly moving UEs. Unlike related works, we take the effect of wind on the propulsion energy consumed by the UAV-BS into account.

The major contributions of our work are summarized as follows. First, we propose the UAV-BS energy consumption model in the presence of wind considering: *i)* the wind speed and wind direction, *ii)* the UAV-BS physical configuration, and *iii)* instantaneous UAV-BS velocity. Second, we predict the sub-optimal trajectory, defined by the circle center, altitude, and flight radius, minimizing the propulsion energy consumption and leveraging the wind via ensemble learning. As shown in [5], hovering with (close to) zero speed results in a significant propulsion energy consumption. Hence, the circular trajectory is commonly considered due to complexity and practical limitations on maneuvering of the UAVs, see, e.g. [5], [8]. Last, we demonstrate a significant propulsion energy saving reached by our proposed algorithm at the cost of negligible capacity degradation compared to the state-of-the-art algorithm maximizing the capacity.

II. System model

In this section, we introduce the generic model of the system, communication model, and wind flow model.

A. Generic model of the system and environment

We consider 3D urban area $\mathcal{A} \subset \mathbb{R}^3$ with buildings. The buildings occupy an area defined by coordinates $\mathcal{A}'$. Furthermore, N UEs are deployed at locations $\mathcal{U} = \{\mathbf{u}_1, \mathbf{u}_2, ..., \mathbf{u}_N\}$, where $\mathbf{u}_n = [x_n, y_n, z_n] \in \mathcal{A}^{\circ}$ for $\forall n \in \langle 1, N \rangle$ and $\mathcal{A}^{\circ} = \mathcal{A} - \mathcal{A}'$ represents the area, where the UEs and the UAV-BSs can move. There are also M static base stations

Manuscript received September XX, 2022; revised September XX, 2022. This work was supported in part by APVV, project number APVV-18-0214, project ITMS2014+: 313011V422, by the European Regional Development Fund, and by the Ministry of Education, Youth and Sports under Grant LTT20004.

Marek Ruzicka and Juraj Gazda are with Technical University of Kosice, Department of Computers and Informatics, Slovakia (e-mail: marek.ruzicka@tuke.sk, juraj.gazda@tuke.sk)

Zdenek Becvar is with Czech Technical University in Prague, Faculty of Electrical Engineering, Technicka 2, 16627 Prague, Czech Republic (e-mail: zdenek.becvar@fel.cvut.cz)

(SBSs) located on the rooftops of the buildings at coordinates $\mathcal{S} = \{\mathbf{s}_1, \mathbf{s}_2, ..., \mathbf{s}_M\}$, where $\mathbf{s}_m = [x_m, y_m, z_m] \in \mathcal{A}'$ for $\forall m \in \langle 1, M \rangle$. Moreover, K UAV-BSs relaying data from the SBSs to the UEs are also deployed in the area at coordinates $\mathcal{D}(t) = \{\mathbf{d}_1(t), \mathbf{d}_2(t), ..., \mathbf{d}_K(t)\}$, where $\mathbf{d}_k(t) = [x_k(t), y_k(t), z_k(t)] \in \mathcal{A}^{\circ}$ for $\forall k \in \langle 1, K \rangle$ at the time t.

Realistic UAV-BSs are limited in maneuvering and their movement should be smooth in terms of direction changes to avoid a high energy consumption [5]. Therefore, we design the circular trajectory, which approximates the optimal trajectory sufficiently with only a minor impact on the performance as demonstrated in [9]. Moreover, a minor deviation in the position of UAV-BSs with respect to an optimal generic shape of the trajectory has only a marginal impact on the capacity of UEs [10]. We consider the circular trajectory with radii $\mathbf{r} = [r_1, r_2, ...r_K]$ at the circle centers $\mathbf{F} = [\mathbf{f}_1, \mathbf{f}_2, \ldots, \mathbf{f}_K] \in \mathcal{R}^{K\times 3}$, where $\mathbf{f}_k = [f_{k,\mathrm{x}}, f_{k,\mathrm{y}}, f_{k,\mathrm{z}}]$. The position of the k-th UAV-BS at the time t is, then, defined as $\mathbf{d}_k(t) = [f_{k,\mathrm{x}} - r_k * \cos\alpha(t), f_{k,\mathrm{y}} - r_k * \sin\alpha(t), f_{k,\mathrm{z}}]$, where $\alpha(t)$ is the relative angle of the UAV-BS to the x-axis.

B. Communication models

We consider orthogonal downlink transmission to the UEs. The capacity of the access channel (superscript a) between the k-th UAV-BS and the associated n-th UE is expressed as

$$C^{\mathrm{a}}_{k,n} = \frac{B}{N}\log_2\left(1 + \frac{P_k g^{\mathrm{a}}_{k,n}\theta^{\mathrm{a}}_{k,n}}{\frac{B}{N}\sigma + I}\right), \quad (1)$$

where B is the available bandwidth distributed equally among N UEs, P_k is the transmission power of the k-th UAV-BS, $g^{\mathrm{a}}_{k,n}$ represents the access channel gain between the k-th UAV-BS and the n-th UE, $\theta^{\mathrm{a}}_{k,n}$ denotes the fading, σ represents the noise density, and I is the interference from neighboring cells.

Analogously, the capacity of the backhaul channel (superscript b) between the m-th SBS and the k-th UAV-BS reserved for data of the n-th UE is defined as

$$C^{\mathrm{b}}_{m,k} = \frac{B}{N}\log_2\left(1 + \frac{P_m g^{\mathrm{b}}_{m,k}\theta^{\mathrm{b}}_{m,k}}{\frac{B}{N}\sigma + I}\right), \quad (2)$$

where P_m is the transmission power of the m-th SBS, $g^{\mathrm{b}}_{m,k}$ is the backhaul channel gain between the m-th SBS and the k-th UAV-BS. We assume the equal bandwidth $\frac{B}{N}$ allocated for all UEs at both access and backhaul channels. This is a reasonable assumption, since the bandwidth does not affect the propulsion energy consumed by the UAV-BS.

For the UAV-BSs' communication, half-duplex decode-and-forward transmission is adopted. Hence, the capacity of the channel between the m-th SBS and the n-th UE via the k-th UAV-BS is determined as

$$C_{m,k,n} = \min(T^{\mathrm{b}}C^{\mathrm{b}}_{m,k}, (1-T^{\mathrm{b}})C^{\mathrm{a}}_{k,n}), \quad (3)$$

where $T^{\mathrm{b}} \in [0,1]$ is the normalized time scheduled for the transmission over the backhaul channel and, analogously, $(1-T^{\mathrm{b}})$ is the normalized time for the transmission over the access channel. To avoid a bottleneck on either of these channels and to maximize $C_{m,k,n}$, we assume [11]

$$C_{m,k,n} = T^{\mathrm{b}}C^{\mathrm{b}}_{m,k} = (1-T^{\mathrm{b}})C^{\mathrm{a}}_{k,n}, \quad (4)$$

The average sum capacity of L UEs served by the k-th UAV-BS and to the m-th SBS over the time τ is defined as

$$\bar{C}_k(\mathbf{f}_k, r_k) = \frac{1}{\tau}\int_0^{\tau} dt \frac{1}{L}\sum_{l=1}^{L}(C_{m,k,l}(\mathbf{d}_k(t))). \quad (5)$$

C. Wind flow model

We model the dynamic effects of the wind via a generally recognized $k-\epsilon$ model based on the Reynolds Averaged Navier-Stokes (RANS) equations [12]. The $k-\epsilon$ model considers the turbulent wind flow, as in an urban environment with multiple obstacles in the wind path and uses time-averaged equations of motion for wind. The wind flow distribution characteristics in the space are, thus, determined by the reference wind distribution vector $\vec{I} = [i_{\mathrm{x}}, i_{\mathrm{y}}, i_{\mathrm{z}}]$ measured at a reference point (RP) randomly selected within the covered area. For each discrete position $a \in \mathcal{A}^{\circ}$, RANS provide an information about the wind velocity $\vec{w_a} = [w_{\mathrm{x}}, w_{\mathrm{y}}, w_{\mathrm{z}}]$. Time evolution of these vectors is expressed as the time evolution of mean velocity vector field (flow velocity) from the left side of the convective form of the RANS equation, as defined in [12]. The $k-\epsilon$ model provides us with the eddy viscosity as a function of the mean flow and solves the RANS closure problem via Boussinesq hypothesis, see [12]. In practice, the model of the environment, where RANS is used to calculate the wind characteristics is described through the finite volume method (FVM) using a mesh. The sensitivity of the mesh η along with the number of iterations ψ determine the accuracy of the model. η and ψ are user-defined specific parameters [13].

The length of UAV-BS operational time ($\sim$ minutes) is sufficiently large compared to the length of turbulent time-scales ($\sim$ milliseconds) presented in the wind flow. In addition, persistent reference wind distribution vector $\vec{I} = [i_{\mathrm{x}}, i_{\mathrm{y}}, i_{\mathrm{z}}]$ is used in RANS. Hence, we can take an advantage of the *wind-flow averaged values* provided by RANS for a prediction of the UAV-BS trajectory instead of the instantaneous values, which are affected by difficult to estimate small-scale turbulence in practice [12].

III. Model of UAV energy consumption with wind

In this section, we introduce a novel model of the propulsion energy consumption for the UAV-BS considering wind.

To derive a model suitable for the wind condition, let us start with the model for the propulsion power consumed at the speed $\tilde{V}$ *without wind*, as introduced in [6]

$$P(\tilde{V}) = \underbrace{P_0\left(1 + \frac{3\tilde{V}^2}{V_{\mathrm{tip}}^2}\right)}_{\text{blade profile}} + \underbrace{P_{\mathrm{i}}\left(\sqrt{1 + \frac{\tilde{V}^4}{4v_0^4}} - \frac{\tilde{V}^2}{2v_0^2}\right)^{1/2}}_{\text{induced}} + \underbrace{\frac{1}{2}d_0\rho s A\tilde{V}^3}_{\text{parasite}}, \quad (6)$$

where P_0, P_{i}, d_0, and s are the UAV hardware specific constants (see [6]), ρ defines the air density, $V_{\mathrm{tip}} = R\omega$ is the tip speed of the rotor blade for the blade angular speed ω

and the rotor radius R, v_0 represents the rotor speed induced by forward flight, and A is the rotor disc area [6].

The model presented in [6] does not consider wind and its impact on the energy consumption. Hence, we include wind-related motion factors into the energy balance in following way. Generally, the wind force F_w actuating on an effective surface A of the UAV is calculated as $F_w = \frac{1}{2}\rho w^2 A$. Let us assume that the wind speed vector $\vec{w}$ results in the active force on the UAV's surface A_ζ perpendicular to the unit normal vector $\vec{e}_\zeta$, which, after substitution, constitutes a generic form of the wind force $\vec{F}_\zeta = \frac{1}{2}\rho(w_\zeta - V_\zeta)^2 \text{sign}(w_\zeta - V_\zeta) A_n \vec{e}_\zeta$. The subscript ζ represents x-, y-, or z-axis. The signum function $\text{sign}(.)$ covers the sign variability with respect to $\vec{e}_\zeta$.

Now, with the above definition of $\vec{F}_\zeta$, the UAV geometry is reducible to a cylindrical symmetry along the vertical z-axis. In this representation sufficient for aerodynamics, the front surface A_f and top/bottom surface A_b are supposed to be the projections of the UAV's surface A_ζ. We further assume the wind speed $\vec{w} = w_\text{x}\vec{e}_\text{x} + w_\text{y}\vec{e}_\text{y} + w_\text{z}\vec{e}_\text{z}$ expressed by means of the orthogonal unit vectors $\vec{e}_\text{x}, \vec{e}_\text{y}, \vec{e}_\text{z}$ representing the components of speed in each axis. By analogy, we suppose that the speed of the UAV in the system related to a ground-based observer is $\vec{V} = V_\text{x}\vec{e}_\text{x} + V_\text{y}\vec{e}_\text{y} + V_\text{z}\vec{e}_\text{z}$. The horizontal speed components V_x and V_y define the respective forces in x and y planes so that:

$$\begin{aligned} \vec{F}_\text{x} &= \frac{1}{2}\rho(w_\text{x} - V_\text{x})^2 \text{sign}(w_\text{x} - V_\text{x}) A_\text{f} \vec{e}_\text{x}\,, \\ \vec{F}_\text{y} &= \frac{1}{2}\rho(w_\text{y} - V_\text{y})^2 \text{sign}(w_\text{y} - V_\text{y}) A_\text{f} \vec{e}_\text{y}\,. \end{aligned} \tag{7}$$

Both forces $\vec{F}_\text{x}$ and $\vec{F}_\text{y}$ then introduce x–y in-plane force $\vec{F}_\text{xy}(t) = \vec{F}_\text{x}(t) + \vec{F}_\text{y}(t)$ actuating on the front surface of the UAV. $\vec{F}_\text{xy}(t)$ represents the horizontal motion with the path with the projection $\vec{s}_\text{xy}(t) = \vec{s}_\text{x}(t) + \vec{s}_\text{y}(t)$. Similarly, the vertical force component $\vec{F}_\text{z} = \frac{1}{2}\rho(w_\text{z} - V_\text{z})^2 \text{sign}(w_\text{z} - V_\text{z}) A_\text{b} \vec{e}_\text{z}$ is proportional to the projection of the bottom (up) surface A_b. The considered model is depicted in Fig. 1.

The total propulsion energy of the k-th UAV-BS $E_k = E_\text{p} + E_\text{f} + E_\text{z}$ is the sum of: *i)* the energy E_p corresponding to the k-th UAV power requirement to maintain motion at the speed V for the total flight time τ, and *ii)* dissipated energy composed of the energy of wind power actuating on the surfaces of the k-th UAV relative to the forces F_xy and F_z for the front and vertical kinetic energies E_f and E_z, respectively.

All three components of the total propulsion energy consumption are computed by time integration of the related powers, i.e., $E_\text{p} = \int_0^\tau dt P(V)$, $E_\text{f} = \int_0^\tau dt \vec{F_\text{xy}}(t) \cdot (\frac{d\vec{s_\text{xy}}(t)}{dt})$ and $E_\text{z} = \int_0^\tau dt \vec{F}_\text{z}(t) \cdot (\frac{d\vec{s}_\text{z}(t)}{dt})$, where $\vec{s}_\text{z}(t)$ represents the pathway projection along $\vec{e}_\text{z}$ to the energy consumption.

IV. Problem Formulation

The objective is to minimize the propulsion energy consumption of the UAV-BSs via a determination of the UAV-BS trajectories. Due to real-world limitations imposed on the trajectories, as explained in Section II, our goal is to determine the circular trajectories including their centers; $\mathbf{F}^* = [\mathbf{f}_1^*, \mathbf{f}_2^*, \dots \mathbf{f}_K^*]$ for all UAV-BSs and respective radii

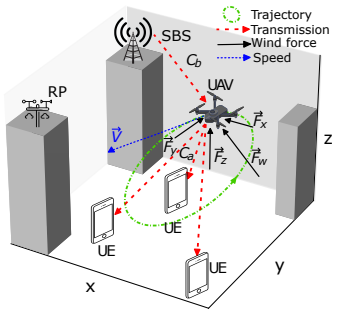

Fig. 1. Model showing wind forces actuating on UAV-BS and speed vector, trajectory, and backhaul/access channels of UAV-BS.

$\mathbf{r}^* = [r_1^*, r_2^*, ..., r_K^*]$. The energy saving optimization problem is, thus, defined as

$$\mathbf{F}^*, \mathbf{r}^* = \underset{\mathbf{F},\mathbf{r}}{\text{argmin}} \sum_{k=1}^{K} E_k, \tag{8}$$

$$\text{s.t. } (\mathbf{f}_k^*) \in \mathcal{A}^\text{o}, \quad \forall k \in \{1, 2, \dots, K\} \tag{a}$$

$$f_{k,z}^* \in \langle z_\text{min}, z_\text{max} \rangle, \quad \forall k \in \{1, 2, \dots, K\} \tag{b}$$

$$r_k^* \in \langle r_\text{min}, r_\text{max} \rangle, \quad \forall k \in \{1, 2, \dots, K\} \tag{c}$$

$$\bar{C}_k^\mathbf{f}(\mathbf{f}_k^*, r_k^*) \geq (1-\gamma)\bar{C}_k^\mathbf{f}(\mathbf{f}_k^{'}, r_k^{'}), \forall k \in \{1, 2, \dots, K\}. \tag{d}$$

The constraint (a) defines the set of all possible locations $\mathcal{A}^\text{o}$ in the area excluding buildings and obstacles, where the presence of UAV-BSs is not allowed. The constraint (b) defines the range of possible UAV-BS altitudes and the constraint (c) defines the range of possible flight radii. The constraint (d) ensures that the average capacity $\bar{C}_k^\mathbf{f}(\mathbf{f}_k^*, r_k^*)$ does not drop below $(1-\gamma)\bar{C}_k^\mathbf{f}(\mathbf{f}_k^{'}, r_k^{'})$, where γ represents the maximum relative allowed decrease in the capacity of UEs with respect to the set of UAV-BSs' positions $\mathbf{F}' = [\mathbf{f}_1^{'}, \mathbf{f}_2{'}, \dots, \mathbf{f}_K{'}]$ and set of radii $\mathbf{r}^{'} = [r_1^{'}, r_2{'}, \dots, r_K{'}]$ maximize the UEs capacity neglecting the energy consumption. Hence, the constraint (d) poses a capacity guarantee on the energy saving optimization problem to ensure the capacity degradation is negligible and within a tolerable limit.

The optimization problem formulated in (8) is typical quadratic programming problem with embedded numerical evaluation of partial differential equations represented by the RANS equation with subject to linear constraints on the variables using FVM. The time complexity of the FVM solution is $\mathcal{O}(\eta \log(\eta))$, where η is the mesh sensitivity characterizing FVM environment. The FVM approximates values by a time evaluation in ψ discrete time steps, so the complexity becomes $\mathcal{O}(\eta \log(\eta)\psi)$ [13]. The cost function in (8) is, thus, extremely computationally expensive, as it includes the evaluation of the UAV-BSs energy consumption in each discrete point of their trajectories by leveraging FVM. Hence, we adopt machine learning to overcome huge complexity and to make the solution feasible for practical applications.

V. Proposed Solution for UAV-BS Trajectory Design with Wind Consideration

In this section, we first determine the theoretical minimum energy consumption. Then, we propose the solution to problem (8). The solution is based on the ensemble learning adopted to

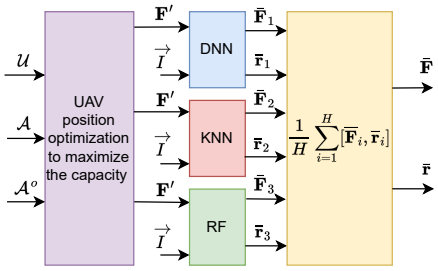

Fig. 2. Ensemble learning approach to determine energy-efficient UAV-BS trajectory. Three base learners (DNN, KNN, RF) are fed with capacity-maximizing UAV-BSs' positions $\mathbf{F}'$ and wind information $\vec{I}$ at the RP.

predict the sub-optimal energy efficient positions of the UAV-BSs $\overline{\mathbf{F}}$ and respective radii $\overline{\mathbf{r}}$.

To identify the theoretical minimum energy consumption of UAV-BSs as defined in (8), we adopt the exhaustive search deriving the optimum $\mathbf{F}^*$ and $\mathbf{r}^*$ by testing all possible options of the UAV-BSs deployment (taking the constraints a, b, and c into account) and selecting the one leading to the minimum energy consumption while fulfilling the capacity constraint d. For practical applications, the exhaustive search is not feasible due to a huge computational complexity. Thus, we also solve (8) as the prediction problem via ensemble learning, where $\mathbf{F}^*$ and $\mathbf{r}^*$ are used only as the targets in the training phase and their computation online is not required.

The ensemble learning typically combines several base learners to improve prediction performance in regression problems compared to standalone predictors. We adopt the heterogeneous set of learners $\mathcal{F}_o = \hat{f}_i,\ i = \{1, 2, \ldots, H\}$, where $H = 3$, as shown in Fig. 2. In the proposed solution, we use a deep neural network (DNN) in combination with traditional random forests (RF) and K-nearest neighbors (KNN) to build heterogeneous ensemble enjoying the benefits of a lower computation cost (shallow DNN and relatively low computing requirements of RF and KNN) and higher diversity potentially leading to a performance improvement [14]. Besides, the individual base learners are characterized by a high sensitivity to the dataset samples and even small changes in the training samples could result in large changes in the predicted output in our problem. However, when combined into the ensemble learning, the base learners are able to produce error lower than that of the single classifier [14].

The feature vector for the ensemble learning is identical for all three base learners and consists of $\mathbf{F}'$, determined via any existing algorithm for positioning of the UAV-BSs to maximize the capacity, and wind information at the RP $\vec{I} = [i_{\mathrm{x}}, i_{\mathrm{y}}, i_{\mathrm{z}}]$. At the deployment stage, the ensemble output is implemented as the average of base learners, i.e., $[\overline{\mathbf{F}}, \overline{\mathbf{r}}] = \frac{1}{H} \sum_{i \in \mathcal{F}} \hat{f}_i[\mathbf{F}', \vec{I}]$.

The hyperparameters of the base learners are identified using the grid-search optimization. The DNN predictor consists of three hidden layers with 30, 40, and 40 neurons respectively, employing ReLU activation function. RF reaches the highest performance, when the number of estimators is set to 160 and the maximum depth equals to 13. For the KNN, the number of neighbors is set to the number of UEs N divided by a desired number of UAV-BSs K.

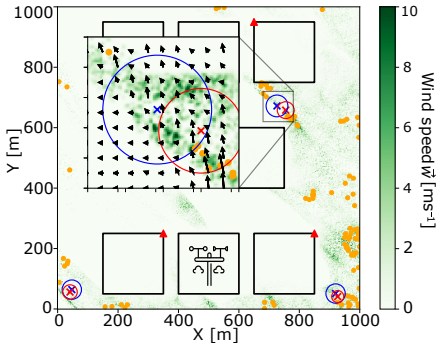

Fig. 3. Example of simulation setup with buildings (black squares), UEs positions (orange dots), SBS positions (red triangles), reference point (RP), capacity-max positions of UAV-BSs derived according to [15] (red crosses and circle trajectory) and UAV-BSs positions computed by the proposed approach (blue crosses and circle trajectory). The wind speed velocity is represented by the green heatmap with zoomed detail encompassing average wind speed vectors at given positions. Note that z-axis omitted for clarity.

VI. Performance Analysis

In our simulation setup, we consider a rectangular urban area with a size of 1×1 km with 8 buildings of different heights. We consider five SBSs located in random positions on the buildings. The UEs are located randomly following the Binomial point distribution. We consider $B = 20$ MHz and spectral density of noise of -174 dBm/Hz. The transmission powers of the SBS and the UAV-BS are equal to 46 dBm and 30 dBm, respectively. Path loss model for line of sight (LoS) channels is in line with [15]. For non-LoS channels, an attenuation of walls/obstacles is added on the top of LoS attenuation as in [15]. Fast fading components are generated as exponentially distributed random variables with unit mean. The simulation outputs are averaged out over 10 000 runs.

The exhaustive search to determine the minimum energy consumption is performed in a discrete space with a step size of 1 m. Finally, the capacity deterioration parameter introduced in (8*d*) is set to $\gamma = 0.03$.

We consider the UAV-BSs represented by the DJI spreading wings S900 model with the shape and HW characteristics given in the specification manual[1]. The visualization of the area considered in our simulation setup is given in Fig. 3.

We compare performance of our proposal with two baseline schemes: *i)* exhaustive search (labeled as *lower-bound*) providing $\mathbf{F}^*$ and $\mathbf{r}^*$, and *ii)* state-of-the-art algorithm maximizing capacity using DNN, as proposed in [15] (labeled as *capacity-max*). Note that the *capacity-max* algorithm does not account for the wind effect in the trajectory design.

As the performance metrics, we adopt the propulsion average energy consumption E as defined in Section III and the sum capacity defined in (5).

Fig. 4a shows notable energy savings of roughly 47% introduced by the proposed approach with respect to the *capacity-max* solution for the average wind speed $|\overline{\vec{w}}| = 10$ ms^{-1} despite the number of UEs deployed in the system. Such savings are expected, since the *capacity-max* does not consider wind in the trajectory design and, hence, the UAV-BSs copes with potentially strong wind forces during flight. The energy

[1] http://dl.djicdn.com/downloads/s900/en/S900_User_Manual_v1.2_en.pdf

saving is almost constant disregarding the number of UEs. The standalone base learners show a slight performance degradation compared to the proposed approach. Hence, a diversity among the base learners results in a superior performance of the proposed ensemble learning. In Fig. 4b, we plot the average sum capacity vs. number of UEs deployed in the system for the average wind speed $\overline{|\vec{w}|} = 10$ ms^{-1}. The proposed solution almost matches the performance of the *capacity-max* algorithm (loss below 0.3%) despite the number of UEs. The standalone base learners show a bit larger performance degradation of about 1.2%, 1.4%, and 2% for DNN, KNN, and RF, respectively.

Furthermore, in Fig. 5a, we show the average propulsion energy consumption over the varying wind speed. The *capacity-max* algorithm with no wind compensation is characterized by an increasing energy consumption with the wind speed. Contrary, our proposed approach and base learners take advantage of the turbulent wind flows by adjusting the trajectories resulting in a decreasing energy consumption with an increasing wind speed. Consequently, the energy saving by our proposal with respect to the state-of-the-art *capacity-max* algorithm becomes more significant with higher wind speed and the proposed approach achieves 47% energy savings for the wind speed $\overline{|\vec{w}|} = 10$ ms^{-1}. Besides, the proposal provides almost identical performance compared to the computationally complex *lower-bound* with difference always below 2%. The energy consumption of the base learners is up to 8% worse compared to the ensemble learning. Finally, in Fig. 5b, we observe the proposed algorithm almost matches (difference below 0.05%) the sum capacity of the *lower-bound* and *capacity-max* across all investigated wind speed characteristics. The base learners show a larger deterioration between 1.37 and 2.75%.

VII. Conclusions

We have introduced new analytical model of the UAV-BS propulsion energy consumption taking the wind into account in order to express the energy consumption at the presence of the turbulent wind flows. Furthermore, we have proposed a novel 3D positioning of UAV-BSs leveraging the wind flow distribution to reduce the propulsion energy consumption. The proposed solution is based on the ensemble learning consisting of three base learners. The simulations show that the proposal reduces the energy consumption significantly (up to 47%) while the sum-capacity is deteriorated only negligibly compared to the state-of-the-art work neglecting the wind.

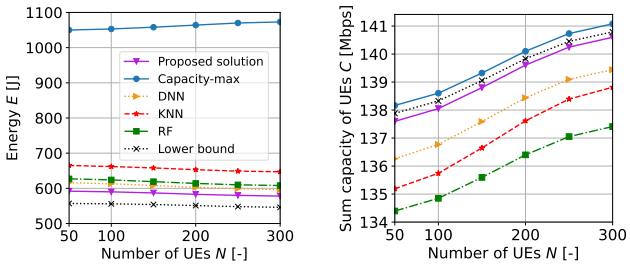

(a) (b)

Fig. 4. Average energy consumption (subplot a) and sum-capacity (subplot b) over varying number of UEs.

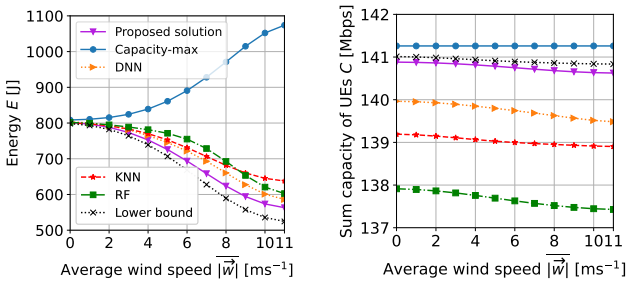

(a) (b)

Fig. 5. Average energy consumption (subplot a) and sum capacity (subplot b) as a function of the average wind speed

References

[1] M. Alzenad, A. El-Keyi, F. Lagum, and H. Yanikomeroglu, "3-D placement of an unmanned aerial vehicle base station (UAV-BS) for energy-efficient maximal coverage," *IEEE Wireless Communications Letters*, vol. 6, no. 4, pp. 434–437, 2017.

[2] L. Wang, B. Hu, and S. Chen, "Energy efficient placement of a drone base station for minimum required transmit power," *IEEE Wireless Communications Letters*, vol. 9, no. 12, pp. 2010–2014, 2020.

[3] L. Li, Q. Cheng, K. Xue, C. Yang, and Z. Han, "Downlink transmit power control in ultra-dense UAV network based on mean field game and deep reinforcement learning," *IEEE Transactions on Vehicular Technology*, vol. 69, no. 12, pp. 15 594–15 605, 2020.

[4] C. Di Franco and G. Buttazzo, "Energy-aware coverage path planning of UAVs," in *2015 IEEE international conference on autonomous robot systems and competitions*. IEEE, 2015, pp. 111–117.

[5] Y. Zeng and R. Zhang, "Energy-efficient UAV communication with trajectory optimization," *IEEE Transactions on Wireless Communications*, vol. 16, no. 6, pp. 3747–3760, 2017.

[6] Y. Zeng, J. Xu, and R. Zhang, "Energy minimization for wireless communication with rotary-wing UAV," *IEEE Transactions on Wireless Communications*, vol. 18, no. 4, pp. 2329–2345, 2019.

[7] Y. Yu, J. Tang, J. Huang, X. Zhang, D. K. C. So, and K.-K. Wong, "Multi-objective optimization for UAV-assisted wireless powered IoT networks based on extended DDPG algorithm," *IEEE Transactions on Communications*, vol. 69, no. 9, pp. 6361–6374, 2021.

[8] P. Beigi, M. S. Rajabi, and S. Aghakhani, "An overview of drone energy consumption factors and models," *arXiv:2206.10775*, 2022.

[9] M. Yang, S.-W. Jeon, and D. K. Kim, "Optimal trajectory for curvature-constrained uav mobile base stations," *IEEE Wireless Communications Letters*, vol. 9, no. 7, pp. 1056–1059, 2020.

[10] Z. Becvar, M. Nikooroo, and P. Mach, "On energy consumption of airship-based flying base stations serving mobile users," *IEEE Transactions on Communications*, 2022.

[11] M. K. Shehzad, A. Ahmad, S. A. Hassan, and H. Jung, "Backhaul-aware intelligent positioning of UAVs and association of terrestrial base stations for fronthaul connectivity," *IEEE Transactions on Network Science and Engineering*, vol. 8, no. 4, pp. 2742–2755, 2021.

[12] T. Kajishima and K. Taira, "Reynolds-Averaged Navier–Stokes Equations," in *Computational Fluid Dynamics*. Springer, 2017, pp. 237–268.

[13] J. Yang, T. Michael, S. Bhushan, A. Hanaoka, Z. Wang, and F. Stern, "Motion prediction using wall-resolved and wall-modeled approaches on a cartesian grid," in *Proc. of the 28th Symposium on Naval Hydrodynamics (USA, Pasadena)*. Citeseer, 2010.

[14] M. A. Ganaie, M. Hu *et al.*, "Ensemble deep learning: A review," *arXiv preprint arXiv:2104.02395*, 2021.

[15] M. Najla, Z. Becvar, P. Mach, and D. Gesbert, "Positioning and association rules for transparent flying relay stations," *IEEE Wireless Communications Letters*, vol. 10, no. 6, pp. 1276–1280, 2021.